Estimation of the lifespan distribution of gold nanoparticles stabilized with lipoic acid by accelerated degradation tests and wiener process

NANO EXPRESS

PAPER

Estimation of the lifespan distribution of gold nanoparticles stabilized with lipoic acid by accelerated degradation tests and wiener process

Betania Sánchez-Santamaría[1], **Boris Mederos**[1], **Delfino Cornejo-Monroy**[1], **Rey David Molina-Arredondo**[1] **and Víctor M Castaño**[2,*]

[1] Instituto de Ingeniería y Tecnología, Universidad Autónoma de Ciudad Juárez, Cd. Juárez, Chih., 32310, México
[2] Centro de Física Aplicada y Tecnología Avanzada, Universidad Nacional Autónoma de México, Querétaro, Qro. 76230, México
* Author to whom any correspondence should be addressed.

E-mail: betania_sanchez@hotmail.com, boris.mederos@uacj.mx, delfino.cornejo@uacj.mx, rey.molina@uacj.mx and vmcastano@unam.mx

Keywords: accelerated degradation tests, gold nanoparticles, life distribution, wiener process

OPEN ACCESS

RECEIVED
1 March 2022

REVISED
2 June 2022

ACCEPTED FOR PUBLICATION
28 June 2022

PUBLISHED
6 July 2022

Abstract

Accelerated degradation tests (ADT) are widely used in the manufacturing industry to obtain information on the reliability of components and materials, by degrading the lifespan of the product by applying an acceleration factor that damage to the material. The main objective is to obtain fast information which is modeled to estimate the characteristics of the material life under normal conditions of use and to save time and expenses. The purpose of this work is to estimate the lifespan distribution of gold nanoparticles stabilized with lipoic acid (GNPs@LA) through accelerated degradation tests applying sodium chloride (NaCl) as an acceleration factor. For this, the synthesis of GNPs@LA was carried out, a constant stress ADT (CSADT) was applied, and the non-linear Wiener process was proposed with random effects, error measures, and different covariability for the adjustment of the degradation signals. The information obtained with the test and analysis allows us to obtain the life distribution in GNPs@LA, the results make it possible to determine the guaranteed time for possible commercialization and successful application based on the stability of the material. In addition, for the evaluation and selection of the model, the Akaike and Bootstrapping criteria were used.

1. Introduction

Accelerated degradation tests (ADT) are an effective tool for evaluating the reliability of materials through the analysis of degradation data, these tests consist of degrading the life of the product by applying a factor that accelerates degradation, thereby obtaining degradation data, which are used to estimate the life distribution of the material under normal conditions of use and at the same time minimize costs and times involved in the test, obtaining good material life data.

For recently created materials, current studies have adopted an ADT in the evaluation of reliability based on the Wiener process. The Wiener process is frequently found in practice as it provides a satisfactory and flexible description of degradation data obtained after having performed an ADT [1, 2].

Nowadays, nanoscience and nanotechnology develop highly innovative materials and products with the ability to revolutionize life as we know it. These nanomaterials, like any other material, show deterioration that involves a very complex interaction between stress, time, and the environment, eventually causing the failure of the product [3]. In this way, in any technological field, knowing the useful life of the products is required for the successful application.

For nanostructured materials, to our knowledge, it has not been determined the life span within an appropriate test time, and the studies found in the literature do not use test methods and degradation analysis to

have reliable information on the life's nanomaterials over the time, moreover, some studies report the need for regulatory reforms to improve supervision of nanomaterials throughout its life cycle [4, 5]. Faced with this condition, there is a wide opportunity of using the ADTs for nanostructured materials to estimate the useful life, as well as, to contribute to the regulation of these materials.

Material of great interest at the nanoscale is gold, which is probably one of the most fascinating materials due to its physical and chemical properties at the nano-scale [6, 7]; gold nanostructures (GNPs) have shown potential applications in many research areas. In medicine, ultra-small nanoparticles below 5 nm have unique advantages in the human body due to their relatively rapid clearance, good absorption, and favorable interaction with radiation [6, 8]. For example, gold nanostructures have been tested as sensors [9] capable of detecting certain diseases such as cancer [10], SARS-CoV-2 [11], Alzheimer's, and Salmonella [9, 10], also, they were utilized as chemical carriers [12, 13] and as theragnostic agents [10, 14].

For the successful application, there is evidence that the stability of gold nanoparticles must be well known to reach the desired tissues or cells [15], overcoming the limitations of biological barriers to diagnose and treat deep targets [8, 16]. Some variables that influence the alteration of stability are the pH [17] of the medium as well as the presence of NaCl [18].

GNPs@LA analyzed in this study are spherical at 2.5 nm, highly stable in colloid as well as a powder; they are stabilized with lipoic acid which prevents agglomeration and creates functional groups for bio-conjugation, and also do not present toxic effects at the cellular level based on ISO 10993–5 [19]. However, there are no studies that allow us to determine the lifetime of the nanomaterial. The purpose of this study is to estimate the failure rate and useful life of GNPs@LA through ADT relied on the Wiener process applying NaCl as an acceleration factor. The proposed methodology is an important contribution to the supply of nanomaterials guarantees and opens the door for the development of further research.

In summary, the main contributions are:

A methodology based on accelerated degradation testing and Wiener process to estimate the useful life of GNPs@LA.

- Estimation of the failure rate GNPs@LA using NaCl as a degradation factor.
- A methodology that relies on a non-linear Wiener process with random effects, error measures, and different covariability to determine the useful life of the GNPs@LA.
- A rigorous statistical analysis to determine the most appropriated Wiener degradation model.

The rest of this paper is structured as follows: section 2 provides a general description of the synthesis and stability of GNP@LA, an explanation of the accelerated degradation model with the Wiener process. Also, it is presented a statistical inference framework based on the maximum likelihood estimation (MLE) method to estimate the parameters of the life distribution. At the end of this section, the statistical framework is applied to our specific degradation problem. Section 3 explores and compares the specified degradation models to our degradation data showing which is the more appropriate model to estimate life distribution. Finally, section 4 gives the conclusions of our work.

2. Materials and methods

2.1. Synthesis of GNPs@LA

Based on the bottom-up approach, particularly the colloidal method; gold nanoparticles with an average size of 2.5 nm were synthesized and stabilized using gold chloride as a precursor, sodium borohydride as a reducer, and lipoic acid as a stabilizer, following the methodology reported by Cornejo-Monroy *et al* [19].

2.2. Stability of GNPs@LA

Gold colloid stability implies that solid nanoparticles do not settle or aggregate at a significant speed [20]. When nanoparticles lose their stability by aggregation, particle size increases and creates agglomerates, losing their interesting properties.

One way to measure how these properties are affected according to their size is through their characterization by UV–vis spectroscopy [21], which is a simple and reliable method to monitor the stability of the gold colloids. As the nanoparticles become destabilized, the original characteristic peak will decrease in intensity due to the depletion of stable nanoparticles, and often the peak will be broadened to longer wavelengths due to the formation of aggregates or agglomerates [22]. The shape and peak position of UV–vis spectra are related to the morphology and size of the nanoparticle, as well as, the dispersion/aggregation of gold colloids [23]. Gold colloids present electronic transitions of bands in the visible range between 450 nm and 550 nm.

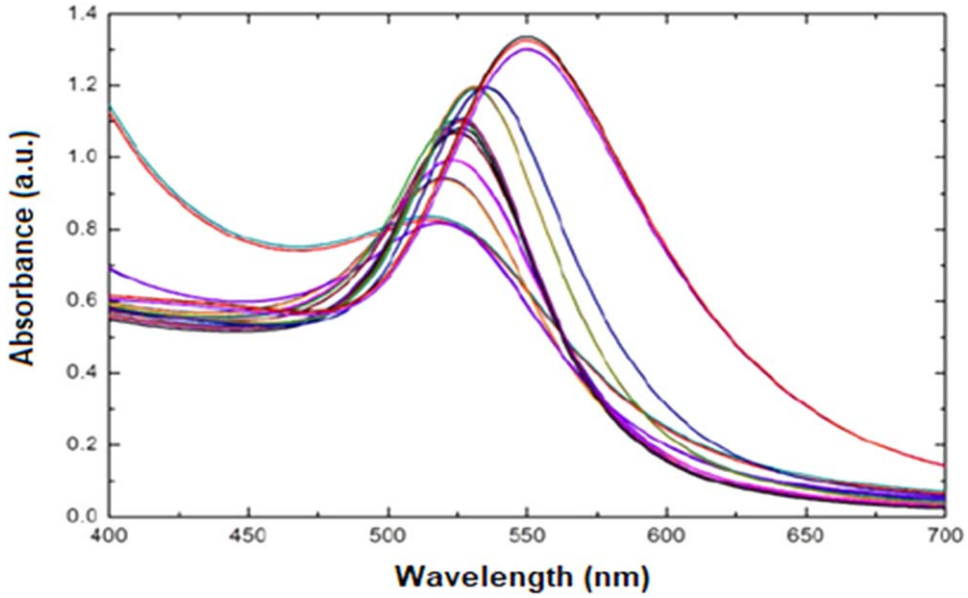

Figure 1. UV–vis absorption spectra of GNPs of 5, 10, 15, 20, 30, 40, 50, 60, and 80 nm in diameter from bottom to top, respectively. Reproduced with permission from J Martínez *et al* [24].

Therefore, some visible wavelengths are absorbed, emitting a characteristic color that can be characterized and related to morphological changes in the nanomaterial [23]. In figure 1, J Martínez *et al* [24] show different sizes of gold nanoparticles as a function of the characteristic peak of the plasmon band, it can be observed that their characteristic peak is red-shift as the GNPs diameter increases. This is because the optical properties of gold nanoparticles change when the particles aggregate and the conduction electrons near the surface of each particle are delocalized and shared among neighboring nanoparticles [25]. When this occurs, the surface plasmon resonance shifts to lower energies, causing the characteristic absorption and scattering peak shift to longer wavelengths [24].

In addition, it is known that charge repulsion effects between particles can be affected by the NaCl concentration of the solution [18]. This occurs because charges can be removed or neutralized by protonated or unprotonated ionizable groups or by the concentration of ions in solution. There is evidence that a high NaCl concentration can effectively mask the charge character of a carboxylate particle by having too many positively charged ions associated with surface charges thus causing aggregates in the material [25].

For this study, and as an example to apply an ADT analysis, to determine the failure rate and useful life of GNPs@LA, we considered that gold nanoparticles with UV–vis spectra peak greater than 525 nm failed and NaCl was used as a factor that accelerates the degradation.

2.3. Accelerated degradation model

One objective of the reliability analysis is to estimate the useful life of the product through the life distribution. To obtain the life distribution of a product using degradation data, the central step is to set up a model that describes the degradation process, called an accelerated degradation model. An accelerated degradation model is the combination of an accelerated model and a degradation model based on physics and statistical models.

An accelerated model shows the relationship between life and effort to establish the connection between degradation data and product life, it is essential to establish a suitable probability model to describe the behavior of collected degradation data, also known as degradation trajectories. Two types of degradation models are commonly used, which are the general trajectory models and the stochastic models.

General trajectory models are described as simple and easy to use, but they lack the ability to capture system dynamics. In contrast, stochastic models have great potential to capture random dynamics within degradation processes. The Wiener process, the Gamma process, and the Inverse Gaussian process are three common stochastic processes that have received many applications in degradation modeling [9, 26]. However, it should be noted that both the Gamma process and the Inverse Gaussian process are only suitable for modeling monotonous degradation trajectories. In comparison, the Wiener process applies to non-monotonous degradation processes that are frequently encountered in practice as it provides a satisfactory and flexible description of the degradation data [2]. The Winner process has been widely applied to degradation data analysis

Table 1. Acceleration models and their link function.

Acceleration model	Link function
Arrhenius Model	$h(S_k) = \exp\left(-\frac{\beta}{S_k}\right)$
Inverse Power	$h(S_k) = \exp(-\beta \ln(S_k))$
Linear Model	$h(S_k) = \exp(-\beta(S_k))$
Quadratic Model	$h(S_k) = \exp(-\beta_1(S_k) + \beta_2(S_k)^2)$

for example to light-emitting diodes [27], fatigue of metals [28], aluminum reduction cells [29], and micro-electromechanical systems [30], among others.

2.4. Wiener degradation process

Since components of systems deteriorate over time and fail when the degradation level reaches a certain threshold. The Degradation information can be measured in a non-destructive way, after which an appropriate degradation model is chosen to describe the process through analysis of the data. Among the degradation models, the Wiener process with positive drift is well-established method due to its mathematical properties, it is expressed as follows,

$$X(t) = \lambda\Lambda(t) + \sigma B(\Lambda(t)), \tag{1}$$

where $\Lambda(t)$ represents the transformed time scale and it is a monotonic continuous function that explains the non-linearization of the data, typical examples are: $\Lambda(t) = e^{bt}$, $\Lambda(t) = blnt$, $\Lambda(t) = t^b$, where $0 < b < 1$ is a parameter to be estimated [31]. The parameters λ and σ stand for the drift and diffusion parameters, respectively. $B(t)$ corresponds to the standard Brownian motion which satisfies the following properties:

i. $B(0) = 0$.

ii. $B(t)$ has normal distribution with mean 0 and variance t.

iii. B(t) has independent increments, for all $t_1 < t_2 < \ldots < t_n$

$$B(t_n) - B(t_{n-1}),\ B(t_{n-1}) - B(t_{n-2}), \ldots, B(t_2) - B(t_1), B(t_1)$$

are independent.

iv. $\{B(t),\ t \geqslant 0\}$ has stationary increments. That is, the distribution of $B(t + s) - B(t)$ does not depend on t.

From the above properties, it can be deduced that random vector $(B(t_1),\ B(t_2),\ \ldots\ , B(t_n)) \sim \mathcal{N}(0,\ \Sigma)$, where the covariance matrix $\Sigma = (\min\{t_i,\ t_j\})_{i,j},\ i,\ j = 1\ ,\ldots,\ n$. The previous properties on $B(t)$ entail that the Wiener degradation process $X(t)$ has the same properties of the Brownian motion $B(t)$ but the first property. Additional is straightforward to see that $X(t) \sim \mathcal{N}(\lambda\Lambda(t),\ \sigma^2\Lambda(t))$.

Due to imperfect instruments, random environments and among other factors, measurements errors are inescapably introduced. Thus, error of measurements ϵ, with $\epsilon \sim \mathcal{N}(0,\ \sigma_\epsilon^2)$ is introduced, leading to an observe degradation process as follows

$$Y(t) = X(t) + \epsilon. \tag{2}$$

Since stress factors such as voltage, humidity, temperature, vibration, etc affect the performance of the degradation process, then an acceleration model can be used to integrate the covariate into the Wiener process. The most common way to incorporate the acceleration model into the Wiener process is to consider some model parameters as a covariate function which is typically called a link function $h(\cdot)$. The choice of the form of this function will depend on the way the acceleration factor influences the model parameters. Some accelerated models are the Arrhenius model, Inverse power model, Eyring model, and linear and quadratic model, which are summarized in the following table 1.

Therefore, the acceleration model of the drift parameter and diffusion parameter depends on the stress factor employing the link function as follows

$$\lambda_k = \eta h(S_k), \quad \sigma_k^2 = \kappa h(S_k), \tag{3}$$

where S_k denotes the stress level and η represents a variability parameter and k is a constant factor associated with the diffusion. From now on $h(S_k)$ will be represented as h_k.

It is common to find differences between the degradation trajectories from unit to unit of the population. This type of difference is the result of non-observable random effects. In order to express this, some model

parameter will be specifics for each unity, obtaining a process with certain parametric distribution [28]. To model this, the drift parameter λ_k will be specific for each unit and follows a normal distribution, on the other hand the parameter σ_k will be taken as a constant, Peng and Tseng [32]. Si *et al* [33, 34] and Tsai *et al* [35]. Thus, it is assumed that the variability parameter η is a random variable with normal distribution $\mathcal{N}(\mu_\eta, \sigma_\eta^2)$. Putting all this together into (2), it is obtained

$$Y_k(t) = Y(t|S_k) = \eta h_k \Lambda(t) + \sqrt{\kappa h_k}\, B(\Lambda(t)) + \epsilon, \tag{4}$$

where (4) models the ADT with random effects, error measurements, and covariates. Some studies that configure more than one variant in the Wiener process, for instance, Li Sun *et al* [36] describe a methodology for the model and estimation of parameters through a constant stress ADT (CSADT) applying the non-linear Wiener process, with covariates, random effects, and measurement errors. A CSADT is a test plan consisting of three to four levels of tests with different proportions of units in each one, where mainly at the low effort level more samples run than at a high level and this type of plan can provide accurate estimates for an ADT. Following the notation in [36], the increasing applied stress level is $S_1, \ldots S_k, \ldots S_K$, where K denotes the maximum stress level. Also, there are N_k units tested under each constant stress S_k and each unit is measured M_{ki} times at the k stress level with $i = 1, 2, \ldots, N_k$. The transformed time will be expressed as $\omega_{kij} = \Lambda(t_{kij})$ with $j = 1,2, \ldots, M_{ki}$.

Therefore, the degradation observed under the Wiener process with its four variants is shown as follows

$$y_{kij}(\omega_{kij}|S_k) = \eta_i h_k \omega_{kij} + \sqrt{\kappa h_k}\, B(\omega_{kij}) + \varepsilon_{kij}, \tag{5}$$

with $\eta_i \sim N(\mu_\eta, \sigma_\eta^2)$, $\varepsilon_{kij} \sim N(0, \sigma_\varepsilon^2)$ and h_k the link function of the accelerated model.

Model (5) comprises the following set of unknown parameters,

$$\boldsymbol{\Theta} = \{\mu_\eta, \sigma_\eta^2, \kappa, \beta, \sigma_\varepsilon^2\} \tag{6}$$

that will be estimated in the next section.

2.5. Statistical inference of the wiener degradation process, parameters estimation, and life distribution on ADT data

In the previous section a model for CSADT was formulated in (5), to estimate the unknown parameters set $\tilde{\boldsymbol{\Theta}}$ let's consider the following vectors $\boldsymbol{T}_{ki} = (t_{ki1}, \ldots, t_{kiM_{ki}})^T$, $t_{kij} = \omega_{kij}$, $\boldsymbol{y}_{ki} = (y_{ki1}, \ldots, y_{kiM_{ki}})^T$, $\boldsymbol{y}_k = (\boldsymbol{y}_{k1}, \ldots, \boldsymbol{y}_{kN_k})^T$ and $\boldsymbol{Y} = (\boldsymbol{y}_1, \ldots, \boldsymbol{y}_K)$ for $k = 1,2, \ldots K$, $i = 1,2, \ldots, N_k$. The properties ii and iii of the Wiener processes implies that the Brownian movement $\boldsymbol{y}_{ki}$ follows a multivariate normal distribution with a mean,

$$\mu_{ki} = \mu_\eta h_k \boldsymbol{T}_{ki} \tag{7}$$

and covariance

$$\boldsymbol{\Omega}_{ki} = \sigma_\eta^2 \tilde{\boldsymbol{\Omega}}_{ki}, \; \tilde{\boldsymbol{\Omega}}_{\boldsymbol{ki}} = \tilde{\mathbf{H}}_{ki} + h_k^2 \boldsymbol{T}_{ki} \boldsymbol{T}_{ki}^{\mathrm{T}},$$

$$\tilde{\mathbf{H}}_{ki} = \tilde{\kappa} h_k \begin{bmatrix} \omega_{ki1} & \omega_{ki1} & \cdots & \omega_{ki1} \\ \omega_{ki1} & \omega_{ki2} & \cdots & \omega_{ki2} \\ \vdots & \vdots & \ddots & \vdots \\ \omega_{ki1} & \omega_{ki2} & \cdots & \omega_{kiM_{ki}} \end{bmatrix} + \tilde{\sigma}_\varepsilon^2 \boldsymbol{I}_{ki} \tag{8}$$

where $\boldsymbol{I}_{ki}$ is the identity matrix of order M_{ki}, where $\tilde{k} = \frac{k}{\sigma_\eta^2}$ and $\tilde{\sigma}_\epsilon^2 = \frac{\sigma_\epsilon^2}{\sigma_\eta^2}$ are a reparameterization to facilitate the inference. The log-likelihood function of unknown parameters $\widetilde{\boldsymbol{\Theta}} = \{\mu_\eta, \sigma_\eta^2, \tilde{\kappa}, \beta, \tilde{\sigma}_\varepsilon^2\}$ is expressed as

$$\begin{aligned} l(\widetilde{\boldsymbol{\Theta}}|\boldsymbol{Y}) \quad = \quad & -\frac{1}{2}\ln(2\pi)\sum_{k=1}^{K}\sum_{i=1}^{N_k} M_{ki} \\ & -\frac{1}{2}\ln(\sigma_\eta^2)\sum_{k=1}^{K}\sum_{i=1}^{N_k} M_{ki} - \frac{1}{2}\sum_{k=1}^{K}\sum_{i=1}^{N_k} ln|\tilde{\boldsymbol{\Omega}}_{ki}| \\ & -\frac{1}{2\sigma_\eta^2}\sum_{k=1}^{K}\sum_{i=1}^{N_k}(\boldsymbol{y}_{ki} - \mu_\eta h_k \boldsymbol{T}_{ki})^T \tilde{\boldsymbol{\Omega}}_{ki}^{-1}(\boldsymbol{y}_{ki} - \mu_\eta h_k \boldsymbol{T}_{ki}). \end{aligned} \tag{9}$$

To estimate the parameters μ_η and σ_η^2, the values of $(\tilde{\kappa}, \beta, \tilde{\sigma}_\varepsilon^2)$ are fixed to specific values, then the derivatives $\frac{\partial l(\tilde{\boldsymbol{\Theta}} \mid \boldsymbol{Y})}{\partial \mu_\eta}$ *and* $\frac{\partial l(\tilde{\boldsymbol{\Theta}} \mid \boldsymbol{Y})}{\partial \sigma_\eta^2}$ of (9) concerning the parameters μ_η and σ_η^2 are computed and equated to zero, obtaining the following close -form expression to the maximum likelihood estimator MLE $\hat{\mu}_\eta$ and $\hat{\sigma}_\eta^2$ of μ_η and σ_η^2

$$\hat{\mu}_\eta = \frac{\sum_{k=1}^{K}\sum_{i=1}^{N_k} h_k \boldsymbol{T}_{ki}^{\boldsymbol{T}} \tilde{\boldsymbol{\Omega}}_{ki}^{-\mathbf{1}} \boldsymbol{y}_{ki}}{\sum_{k=1}^{K}\sum_{i=1}^{N_k} h_k^2 \boldsymbol{T}_{ki}^{\boldsymbol{T}} \tilde{\boldsymbol{\Omega}}_{ki}^{-\mathbf{1}} \boldsymbol{T}_{ki}} \tag{10}$$

$$\hat{\sigma}_{\eta}^{2} = \frac{1}{\sum_{k=1}^{K}\sum_{i=1}^{N_k} M_{ki}} \sum_{k=1}^{K}\sum_{i=1}^{N_k} (\boldsymbol{y}_{ki} - \hat{\mu}_{\eta} h_k \boldsymbol{T}_{ki})^{T} \tilde{\boldsymbol{\Omega}}_{ki}^{-1} (\boldsymbol{y}_{ki} - \hat{\mu}_{\eta} h_k \boldsymbol{T}_{ki}). \tag{11}$$

Substituting (10) and (11) in (9) and simplifying the log-likelihood function, it is obtained

$$l(\tilde{\boldsymbol{\Theta}}|\boldsymbol{Y}) = -\frac{1}{2}(\ln(2\pi) + 1)\sum_{k=1}^{K}\sum_{i=1}^{N_k} M_{ki}$$
$$-\frac{1}{2} ln(\hat{\sigma}_{\eta}^{2})\sum_{k=1}^{K}\sum_{i=1}^{N_k} M_{ki} - \frac{1}{2}\sum_{k=1}^{K}\sum_{i=1}^{N_k} ln|\tilde{\mathbf{H}}_{ki} + h_k^{2}\boldsymbol{T}_{ki}\boldsymbol{T}_{ki}^{\mathrm{T}}|. \tag{12}$$

Note that the matrix $\tilde{\mathbf{H}}_{ki}$ depends on the parameters $\tilde{\kappa}$, β and $\tilde{\sigma}_{\varepsilon}^{2}$ and h_k^{2} depends on β. Therefore, the maximum likelihood estimates of $\tilde{\kappa}$, β, $\tilde{\sigma}_{\varepsilon}^{2}$ can be obtained by maximizing the log-likelihood function (12) by employing the L-BFGS-B quasi-Newton optimization method that can be found in the R-project packages [37]. The value of $\hat{\kappa}$ can be obtained by the following equations:

$$\hat{\kappa} = \quad \hat{\tilde{\kappa}} \cdot \hat{\sigma}_{\eta}^{2}, \tag{13}$$

$$\hat{\sigma}_{\varepsilon}^{2} = \hat{\tilde{\sigma}}_{\varepsilon}^{2} \cdot \hat{\sigma}_{\eta}^{2}, \tag{14}$$

One objective of the reliability analysis is to estimate the useful life of the product through the life distribution. To obtain the life distribution of a product using degradation data Li *et al* [31] incorporate the measurement errors into the deduction of the expression for the CDF and PDF of the failure time

$$T = inf\{t: \quad Y(t) \geqslant w\}, \tag{15}$$

where T corresponds to the first time that the degradation process Y hits a failure threshold w. They deduced the life PDF expression for each stress level S_k, which can be found in equation (12) at [31] Note that in this formulation they used two different time scales $\Lambda(t)$ and$\tau(t)$, when $\tau(t) = \Lambda(t)$, this PDF is reduced to,

$$f_{S_k}(t) = \frac{\sigma_{\varepsilon}^{2} h_k \mu_{\eta} + (\kappa h_k + h_k^{2}\sigma_{\eta}^{2})w}{\sqrt{2\pi(h_k\omega(\kappa + h_k\sigma_{\eta}^{2}\omega) + \sigma_{\varepsilon}^{2})^{3}}} \cdot \frac{d\omega}{dt} \cdot \exp\left\{\frac{-(w - h_k\mu_{\eta}\omega)^{2}}{2(h_k\omega(\kappa + h_k\sigma_{\eta}^{2}\omega) + \sigma_{\varepsilon}^{2})}\right\} \tag{16}$$

which is the one used in this work. Note $f_{S_k}(t)$ depends on the parameters set $\tilde{\boldsymbol{\Theta}}$.

2.6. Methodology and analysis of degradation data under the wiener process/ADT

To obtain degradation data of GNPs@LA under a CSADT, several samples were synthesized following the methodology reported by Cornejo *et al* [19] and using NaCl as an acceleration factor. The stress test levels were based on an exploratory study, leaving three different levels of effort for three different populations. UV–vis absorption spectra of colloids were carried out every third-day generating degradation signals for low, medium, and high levels. In this study, the material degradation was determined considering the absorbance between 450 and 550 nm, and the maximum characteristic peak of gold. Gold colloids with a characteristic peak greater than 525 were considered as a failure.

Since this work proposes to estimate the life distribution of GNPs@LA applying a CSADT. Accordingly, the following can be defined:

- The percentage levels of NaCl are indexed as $k = 1, \ldots, K$
- The population of samples is indexed as $i = 1, \ldots, N_k$
- Measurement times are indexed as $j = 1, \ldots, M_{ki}$

  Once the degradation signals have been defined as degradation data, we proceed to obtain the configuration of the CSADT that describes the degradation trajectories. Thus, this work proposes the non-linear Wiener process with drift parameter, random effects, measurement errors, and different link functions in the covariability (table 1, section 2.3) is used. More specifically the model assumes:
- A drift parameter with transformed times $\omega_{kij} = \Lambda(t_{kij}) = (t_{kij})^{b}$ that explain the non-linearity of the data.
- Random effects in the drift parameter. Different units have different drift parameters while all diffusion parameters have the same value under a certain effort. So, the parameter η in the drift term at (5) is assumed to has a normal distribution $\eta \sim N(\mu_{\eta}, \sigma_{\eta}^{2})$.
- Measurement errors with $\varepsilon_{kij} \sim N(0, \sigma_{\varepsilon}^{2})$.
- Covariability, which is expressed via the link function h_k, where the accelerated model is immersed. It is

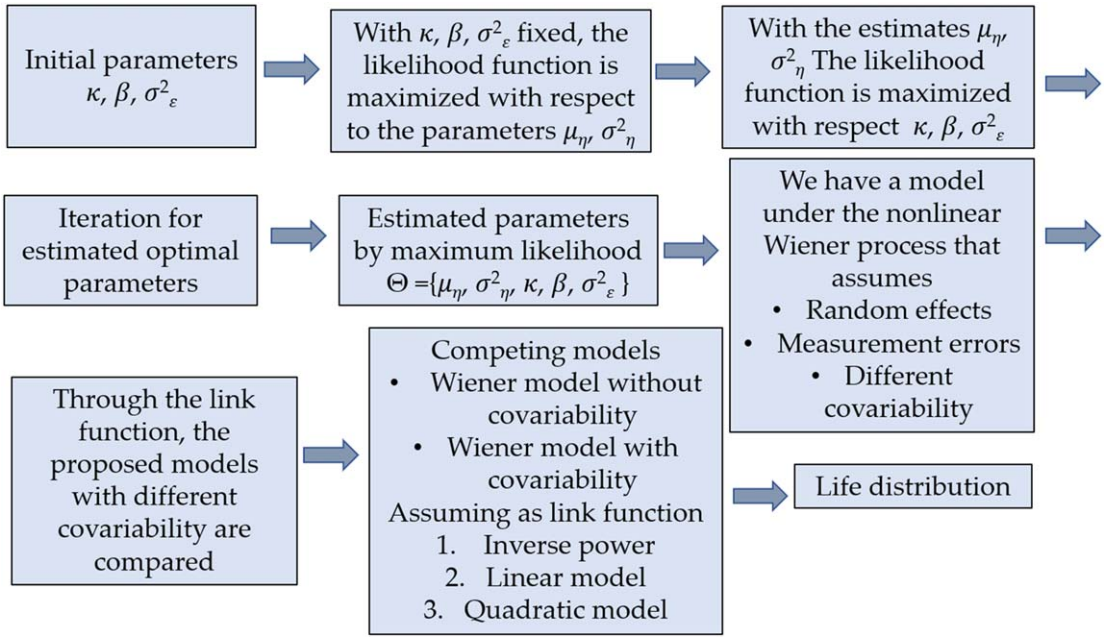

Figure 2. Methodology for the estimation of parameters in the proposed models.

highlighted three accelerated models that were evaluated in this work corresponding, inverse power, linear model, and the quadratic model, see (table 1, section 2.3).

Now, proposing the CSADT and the Wiener process with these characteristics, the degradation process can be established as formula (5). Thus, the following parameter set $\tilde{\Theta} = \{\mu_\eta, \sigma^2_\eta, \tilde{\kappa}, \beta, \tilde{\sigma}^2_\varepsilon\}$ will be estimated to get the life distribution. We remark that $\beta = (\beta_1, \beta_2)$ in the quadratic model case and $\beta = \beta_1$ in the remaining cases.

All the above were programmed in the statistical software R, where the MLE was applied to obtain the parameters set $\tilde{\boldsymbol{\Theta}}$. Figure 2 shows the proposed methodology.

As can be seen in figure 2, different degradation models have been proposed. To select the best model will be used the AIC criterion [38] and for the evaluation and validation, the estimated parameters of the model will be employed and the Bootstrapping distribution [39] will be calculated with the construction of confidence intervals.

3. Results

The constant stress ADT in GNPs@LA had 3 levels, these being: 19 samples for the low level with 8% NaCl, 13 samples for the medium level with 12%, and 12 samples for the high level with 16% NaCl m/v. With a censorship time of 69 days; except for the low level which was 51 due to remaining time conditions and modifications of the plan. The degradation measurements were performed every third day generating a total of 18 measurements for low level and 23 measurements for medium level and high level, providing degradation signals over time.

From UV–vis absorption spectra degradation signals were obtained. In figure 3, the changes in the spectra are graphically presented comparing the first measurement and the last measurement in the range of 400 to 800 nm in wavelength.

It can be observed in figure 3 that for the three degradation levels, the absorbance amplitude decreases, and the width of the band broadens causing a red-shifted of the characteristic peak due to their increase in size and the aggregation of the gold nanoparticles. It can be also noticed that at higher percentages of NaCl the degradation is more appreciable than at lower percentages. To have a better relationship between UV–vis spectra and degradation material we made a graph from the initial average and final characterization for each level, which can be seen in figure 4. The area comprised between 450 and 550 nm from UV–vis spectra was used to quantify the material degradation. Additionally, when the characteristic peak moves above 525 nm is considered the failure threshold.

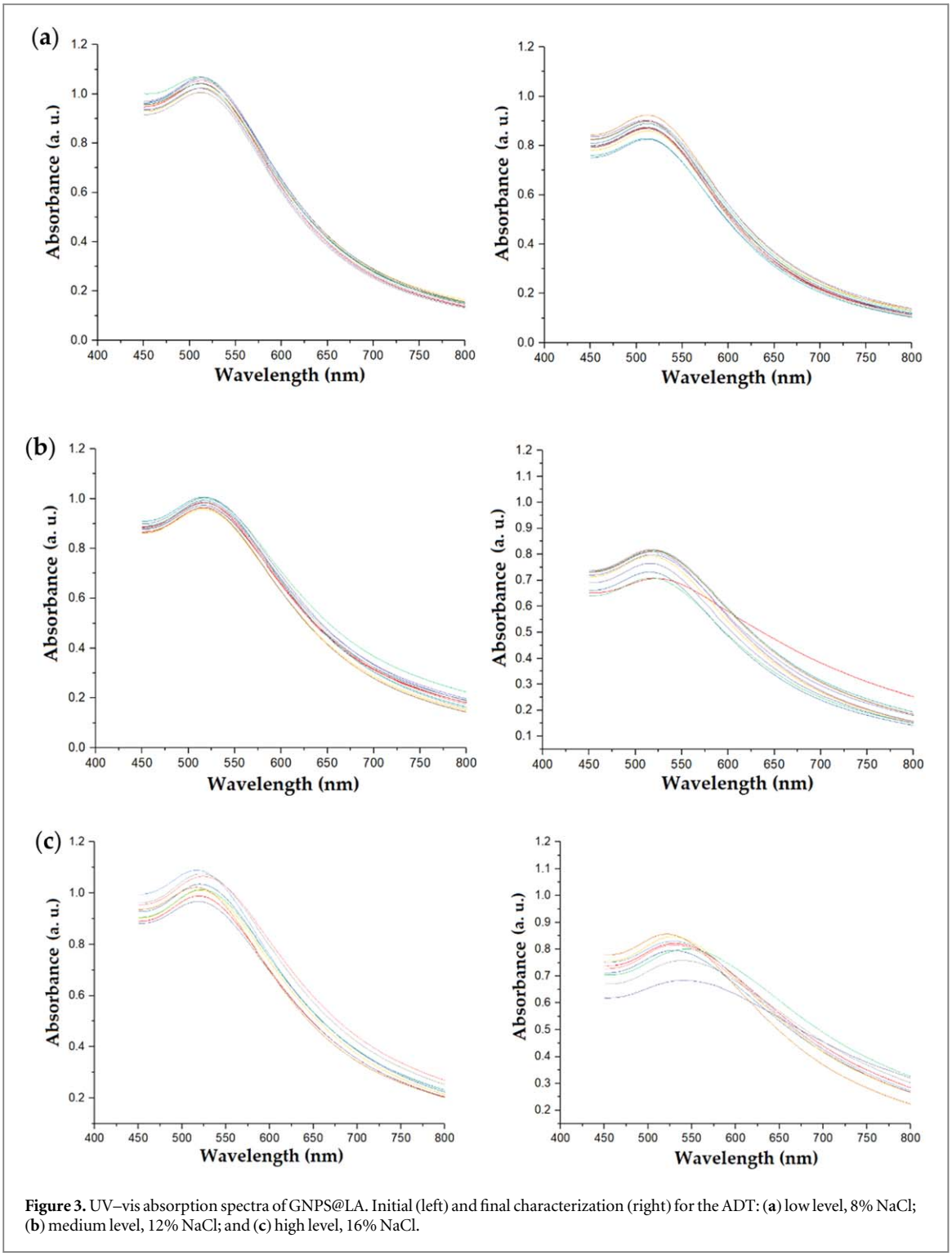

Figure 3. UV–vis absorption spectra of GNPS@LA. Initial (left) and final characterization (right) for the ADT: (**a**) low level, 8% NaCl; (**b**) medium level, 12% NaCl; and (**c**) high level, 16% NaCl.

From figure 4, a change in the area between the initial and final characterization is well noted and it was used to obtain degradation data.

To maintain a notation according to the property of independent increments and a normal distribution under the Wiener process, the area for each measurement was calculated, and each degradation increment was obtained from the difference between the first-day area and the subsequent day areas, these were the increments of degradation to be modeled. Under this consideration, the degradation trajectories were obtained for each sample at the different levels of NaCl.

In figure 5 the different trajectories at each level are shown, it can also be observed that there is a non-monotonous behavior with increasing and decreasing trends. Also, it is observed that the degradation of gold colloids with the same levels of NaCl is different, this can be attributed to unobservable factors such as concentration, unit-to-unit variability, inherent randomness, as well as the measurement variability of each

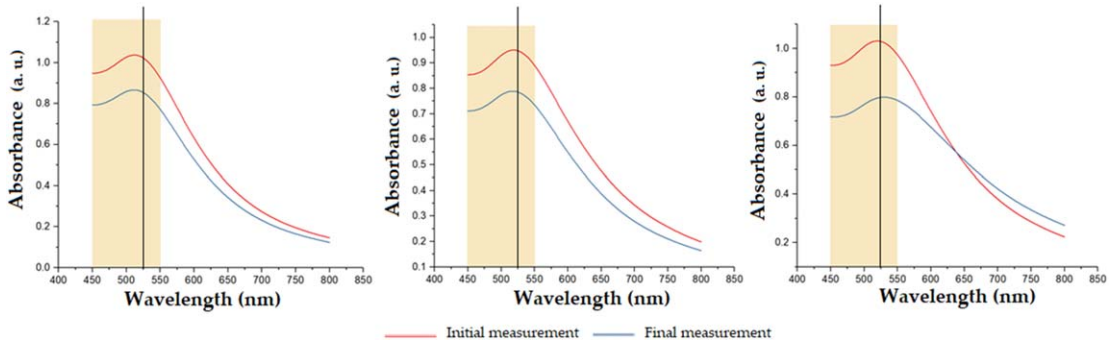

Figure 4. Average UV–vis absorption spectra from the initial and final characterization for each level of the ADT. From left to right: low, medium, and high level, respectively.

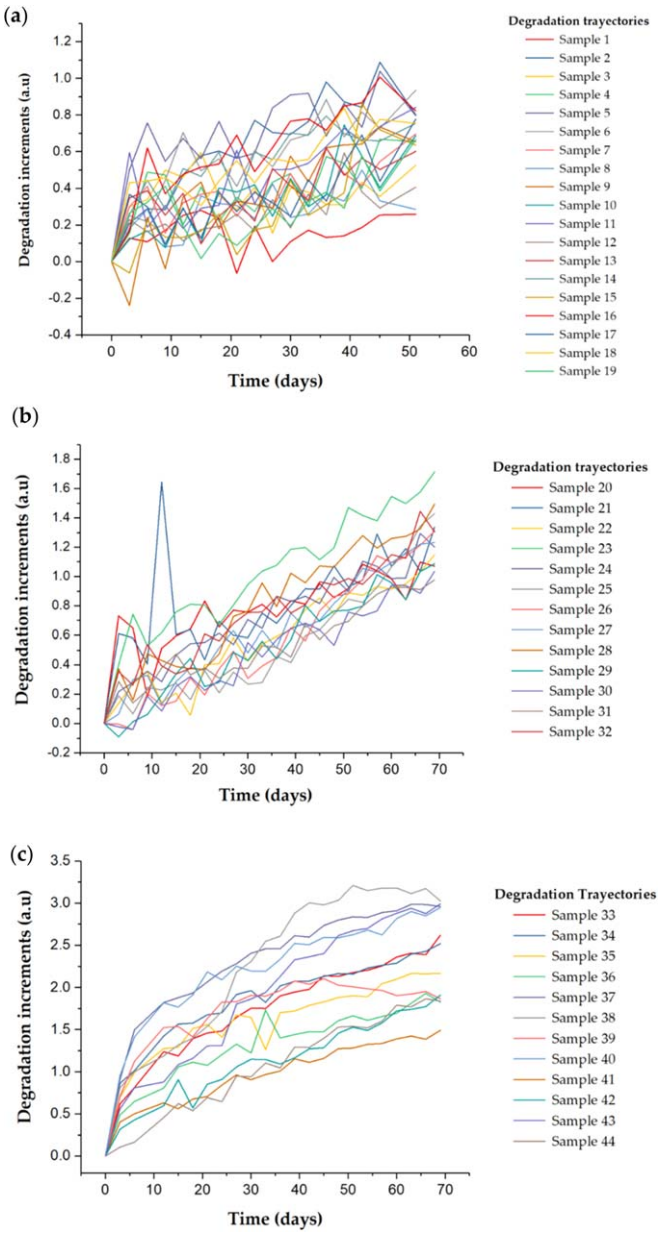

Figure 5. Degradation trajectories of GNPs@LA with size of 2.5 nm for the different levels of NaCl: (**a**) low level, 8% NaCl; (**b**) medium level, 12% NaCl; and (**c**) high level, 16% NaCl.

Table 2. Obtained Optimal parameters for each accelerated degradation model.

Covariability	Optimal parameters				
	μ_η	σ_η^2	κ	β	$\tilde{\sigma}_\eta^2$
Inverse Power	0.00251	4.0E-08	0.00028	−1.4986	0.00801
Linear Model	0.01741	2.0E-07	0.00181	−0.1428	0.00849
Quadratic Model	0.04386	6.4E-06	0.00460	(0.014, 0.0062)	0.00838

sample. Thus, the Wiener stochastic model was chosen with its four variants since it has great potential to capture stochastic dynamics, and it is also applicable to non-monotonic impairments, providing a satisfactory and flexible description of the impairment data.

For this study, we propose to model the degradation trajectories under the non-linear Wiener process, with random effects, error measurements, and different covariability using three different link functions, which generate three different models.

To obtain the optimal parameters in each model, the initial parameters should be close to the true model parameter to be estimated, as well as the value b in the time transformation, these were obtained by a preliminary package made by us using RStudio that performs an individual regression using least squares for each degradation path giving as initial parameters $b = 0.61$, $\tilde{\kappa} = 0.65$, $\beta = -0.8479$, $\tilde{\sigma}_\varepsilon^2 = .01$ assuming inverse power, for a linear model they were $b = 0.61$, $\tilde{\kappa} = 0.65$, $\beta = -0.18$, $\tilde{\sigma}_\varepsilon^2 = .01$ and finally for a quadratic model the initial parameter were $b = 0.61$, $\tilde{\kappa} = 0.65$, $\beta_1 = 0.04$, $\beta_2 = 0.1$ $\tilde{\sigma}_\varepsilon^2 = .01$. Once these initial parameters were estimated, they were fixed at the likelihood function to estimate the optimal values of μ_η *and* σ_ε^2 via the MLE approach (in closed form (10) and (11)) presented in section 2.4. Scale time transformation parameter was remained fixed at $b = 0.61$ during optimization and to avoid over-estimation parameter β_2, the constraint $\mu_\eta h_k > \mu_\eta h_{k+1}$ for $k > 1$ was added in the quadratic model. The obtained optimal parameters are highlighted in table 2.

With the estimated parameters of the model in table 2 and establishing w as the failure threshold, which corresponds to a 1.51 degradation increment, equivalent to an area of 2.1 units implying a 525 nm deface in the wavelength. The life distribution is given by (16). Therefore, the density and cumulative density functions for each degradation level are shown in figure 6. It is observed that at higher percentages the degradation is more noticeable, also the probability mass concentrates more towards zero as the percentage of NaCl increases, according to the accelerated degradation test.

Given the cumulative density of the model, this can be evaluated to make desired inferences and consequently estimate the useful life under different conditions. As an example of this, table 3 presents some failure rates based on formula (16).

As can be seen in table 3, the results between different models differ, being the quadratic model, which provides the lowest failure rate.

To select the best model, the Akaike information criterion (AIC) introduced by Hirotugu Akaike in 1973 has been one of the most widely known and used model selection tools with degradation forecast [38]. This criterion has been used by some authors such as [40–42] for the selection of the most appropriate degradation model given a set of degradation measures. The AIC is used as a selection criterion when the model parameters have been estimated by maximum likelihood, its formula is given by

$$AIC = -2\log L + 2p, \tag{17}$$

where $\log L$ is the log likelihood and p is the number of parameters in the model, the likelihood function reflects the conformity of the model with the observed data, the higher the conformity between the model and the data the higher the likelihood, however, when the number of model parameters increases the likelihood usually increases so the AIC penalizes the number of parameters. Therefore, the selected model will be the one with a minimum AIC. According to the above explanation, we will use the AIC to establish the covariability influences. Modeling without covariance yields an AIC value of −931,703 which is higher compared to the AIC values for the proposed models, as can be seen in table 4.

It can be easily seen that covariability has an influence on the models and must be embedded in the process. The application of the AIC criterion suggests that the quadratic model is a better option for the degradation data obtained.

Continuing with the assessment, the bootstrap method [43] is used to determine confidence interval (CI) for the failure distribution, the CI is found by using the estimated model parameters with the sample data as if they were the true parameters, since this is the information available from the degradation process. New degradation samples are generated from the estimated parameters, with these data, new model parameters are estimated and

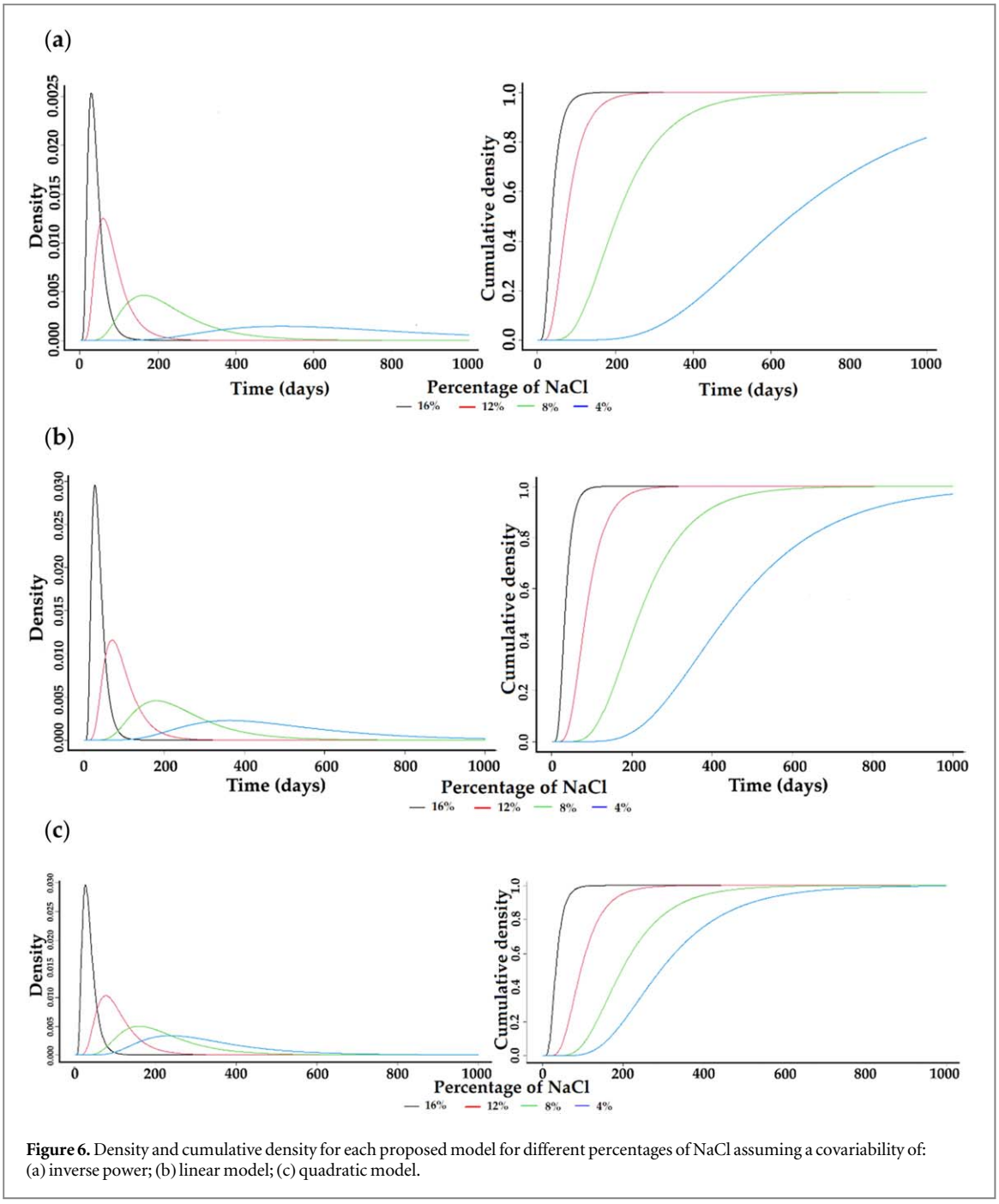

Figure 6. Density and cumulative density for each proposed model for different percentages of NaCl assuming a covariability of: (a) inverse power; (b) linear model; (c) quadratic model.

used to obtain a new cumulative failure distribution. It is necessary to repeat the above procedure many times, thus obtaining an approximation to the sampling distribution. It is common to plot the empirical distribution of the failure pseudo-times with the confidence intervals to check the adequacy of the model, the more pseudo-times are within the confidence intervals the higher the adequacy. The Bootstrap was applied using 4000 datasets. The results are shown in figure 7 for each model.

According to the obtained CIs with a confidence level of 95% which are observed in figure 7, the percentages of 8% and 16% present an empirical value which is closed to the theoretical cumulative density. On the other hand, it can be noted that at 12% percentage the three models present several distant points outside the CI, however, the quadratic model seems to have more values within the confidence interval, as well as close to the theoretical distribution.

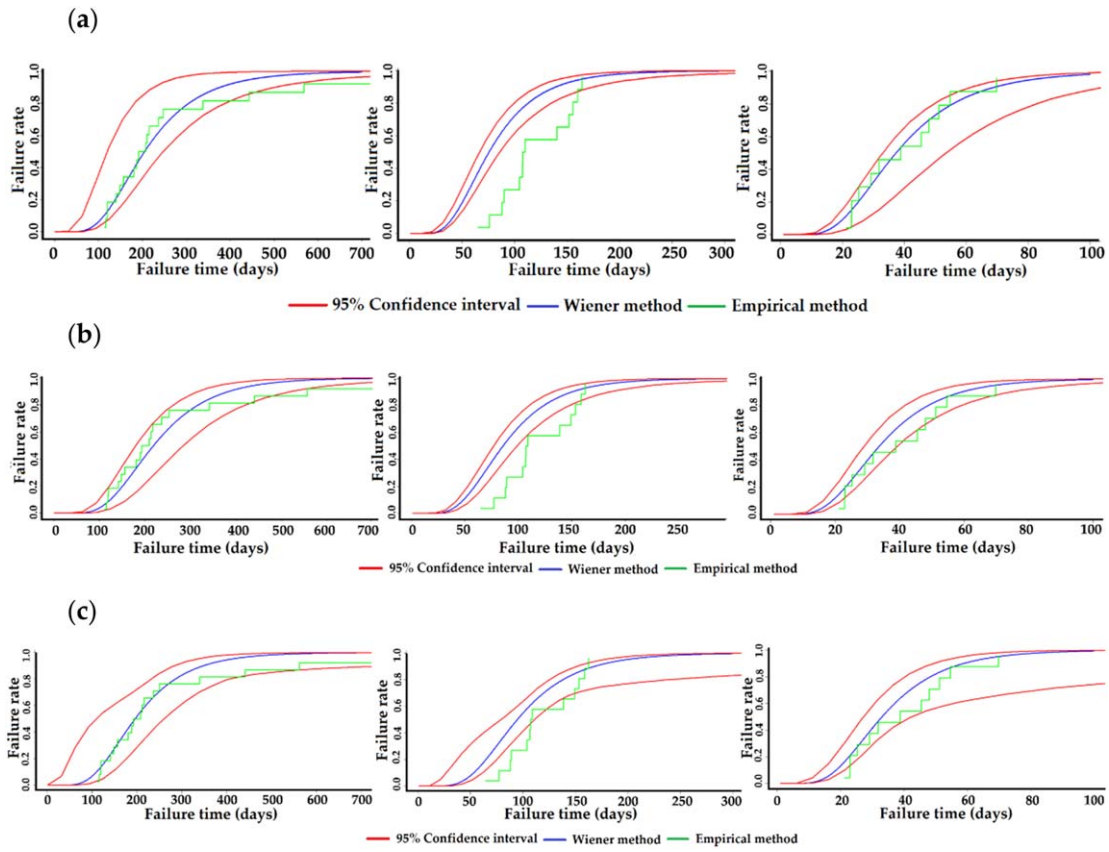

Figure 7. Bootstrap results for each degradation model using NaCl at 8%, 12% and 16%, from left to right. (a) Inverse power model; (b) Linear model; (c) Quadratic model.

Table 3. The Failure rate in gold colloids with different NaCl percentages and covariability was obtained by the three proposed models.

Days	Inverse power model								
	0%	1%	5%	8%	10%	12%	15%	16%	20%
30	Undefined	0.000	0.000	0.000	0.001	0.023	0.211	0.321	0.756
72	Undefined	0.000	0.000	0.012	0.144	0.457	0.853	0.916	0.994
360	Undefined	0.000	0.103	0.882	0.990	0.999	1.000	1.000	1.000
720	Undefined	0.002	0.585	0.996	1.000	1.000	1.000	1.000	1.000
1080	Undefined	0.013	0.857	1.000	1.000	1.000	1.000	1.000	1.000
	Linear model								
	0%	**1%**	**5%**	**8%**	**10%**	**12%**	**15%**	**16%**	**20%**
30	0.000	0.000	0.000	0.000	0.000	0.009	0.216	0.399	0.971
72	0.000	0.000	0.000	0.006	0.073	0.346	0.886	0.960	1.000
360	0.001	0.020	0.322	0.872	0.987	1.000	1.000	1.000	1.000
720	0.062	0.315	0.868	0.997	1.000	1.000	1.000	1.000	1.000
1080	0.268	0.669	0.980	1.000	1.000	1.000	1.000	1.000	1.000
	Quadratic model								
	0%	**1%**	**5%**	**8%**	**10%**	**12%**	**15%**	**16%**	**20%**
30	0.000	0.000	0.000	0.000	0.000	0.005	0.191	0.413	0.998
72	0.000	0.000	0.001	0.013	0.065	0.270	0.859	0.958	1.000
360	0.622	0.611	0.733	0.913	0.981	0.999	1.000	1.000	1.000
720	0.969	0.966	0.985	0.998	1.000	1.000	1.000	1.000	1.000
1080	0.997	0.997	0.999	1.000	1.000	1.000	1.000	1.000	1.000

Table 4. AIC criterion values for the different models considering covariability.

Inverse power model	Linear model	Quadratic model
−993.771	−997.439	−998.017

4. Discussion

The results of the research show that according to the AIC criterion and the bootstrap confidence interval the quadratic acceleration model has a better adjustment of the degradation of the GNPs@LA, however, in the ADT and ALT the samples usually show a degree of curvature that is not sufficient for the AIC criterion to better consider the quadratic acceleration model over a linear one. In our model, the curvature was large enough to improve the AIC criterion. When a curvature parameter is added in an ADT, special attention should be paid, since there could be an overestimation of the degradation of the product under normal conditions of use, to avoid this overestimation we add the restriction $\mu_\eta h_k > \mu_\eta h_{k+1}$ for $k > 1$ in the estimation of the model parameters, thus obtaining an estimate of the failure fraction of the GNPs@LA under normal conditions of use consistent with the little knowledge that we had of them. We also recommend further investigation of the quadratic acceleration model in ADT tests.

5. Conclusions

This research proposed a methodology and an analysis model to estimate the failure rate and useful life of GNPs@LA based on accelerated degradation tests and a non-linear Wiener process incorporating random effects, error measures, and covariability. The proposed scheme employs three different link functions in covariability using the inverse power, linear and quadratic models.

The modeling has been tested using NaCl as an acceleration factor and a three-level constant stress ADT with 8%, 12%, and 16% of NaCl as degradation signals and as degradation data in the Wiener process. The data presented a non-monotonous behavior with oscillatory tendencies, and the GNPs@LA degradation observed for the same population was different thus the Wiener stochastic process was applied with its four variants.

It is demonstrated that the model applied by the non-linear Wiener process, with random effects, error measures, and covariability that uses the quadratic model as a link function was the most effective and gives the best estimate of the degradation rate of the shelf life of GNP@LA and as a function of NaCl. These results can be used to provide guarantees of commercially available nanomaterials.

Acknowledgments

The authors wish to express the acknowledgment to CONACYT that supported this research.

Data availability statement

All data that support the findings of this study are included within the article (and any supplementary files).

Author contributions

Conceptualization, B.S.-S., B.M., D.C.-M., and R.M.-A.; methodology, B.S.-S., B.M., D.C.-M., and R.M.-A.; software, B.S.-S., B.M., D.C.-M., and R.M.-A.; writing-original draft preparation, B.S.-S., B.M., D.C.-M., and R.M.-A.; validation, B.S.-S., B.M., D.C.-M., and R.M-A; formal analysis, B.S.-S., B.M., D.C.-M., R.M.-A. and V.C.-M.; investigation, B.S.-S., B.M., D.C.-M., R.M.-A. and V.C.-M.; data curation, B.S.-S., B.M., D.C.-M., and R.M.-A.; writing—review and editing, B.S.-S., B.M., D.C.-M., R.M.-A. and V.C.-M.; supervision, B.S.-S., B.M., D.C.-M., R.M.-A. and V.C.-M.; project administration, B.S.-S., B.M., D.C.-M., R.M.-A. and V.C.-M.; funding acquisition, B.S.-S., B.M., D.C.-M., R.M.-A. and V.C.-M. All authors have read and agreed to the published version of the manuscript.

Funding

This research received no external funding.

Institutional Review Board Statement

Not applicable.

Informed consent statement

Not applicable.

Conflict of interest

The authors declare no conflict of interest, whatsoever.

ORCID iDs

Betania Sánchez-Santamaría https://orcid.org/0000-0002-5014-8797
Delfino Cornejo-Monroy https://orcid.org/0000-0002-6294-7385
Víctor M Castaño https://orcid.org/0000-0002-2983-5293

References

[1] Ye Z-S and Xie M 2015 Stochastic modelling and analysis of degradation for highly reliable products *Applied Stochastic Models in Business and Industry* **31** 16–32
[2] Zhang Z, Si X, Hu C and Lei Y 2018 Degradation data analysis and remaining useful life estimation: a review on Wiener-process-based methods *Eur. J. Oper. Res.* **271** 775–96
[3] Cornejo-Monroy D, Acosta-Torres L S, Moreno-Vega A I, Saldana C, Morales-Tlalpan V and Castaño V M 2013 Gold nanostructures in medicine: past, present and future *J Nanosci Lett* **3** 1–9
[4] Larsson S, Jansson M and Boholm Å 2019 Expert stakeholders' perception of nanotechnology: risk, benefit, knowledge, and regulation *J. Nanopart. Res.* **21** 57
[5] Saldivar-Tanaka L 2018 Regulando la nanotecnología *Mundo Nano. Revista Interdisciplinaria en Nanociencias y Nanotecnología* **12** 37–57
[6] Haume K, Rosa S, Grellet S, Śmiałek M A, Butterworth K T, Solov'yov A V, Prise K M, Golding J and Mason N J 2016 Gold nanoparticles for cancer radiotherapy: a review *Cancer Nanotechnol.* **7** 8
[7] Tamayo L, Palza H, Bejarano J and Zapata P A 2019 Polymer composites with metal nanoparticles: synthesis, properties, and applications *In Polymer Composites with Functionalized Nanoparticles* ed K Pielichowski and T M Majka (Elsevier) 249–86
[8] Huang K *et al* 2012 Size-dependent localization and penetration of ultrasmall gold nanoparticles in cancer cells, multicellular spheroids, and tumors *in vivo ACS Nano* **6** 4483–93
[9] Afonso A S, Pérez-López B, Faria R C, Mattoso L H C, Hernández-Herrero M, Roig-Sagués A X, Maltez-da Costa M and Merkoçi A 2013 Electrochemical detection of Salmonella using gold nanoparticles *Biosens. Bioelectron.* **40** 121–6
[10] Guo J, Rahme K, He Y, Li L L, Holmes J D and O'Driscoll C M 2017 Gold nanoparticles enlighten the future of cancer theranostics *Int J Nanomedicine* **12** 6131–52
[11] Sivasankarapillai V S, Pillai A M, Rahdar A, Sobha A P, Das S S, Mitropoulos A C, Mokarrar M H and Kyzas G Z 2020 On facing the SARS-CoV-2 (COVID-19) with combination of nanomaterials and medicine: possible strategies and first challenges *Nanomaterials* **10** 852
[12] Daraee H, Eatemadi A, Abbasi E, Fekri Aval S, Kouhi M and Akbarzadeh A 2016 Application of gold nanoparticles in biomedical and drug delivery *Artificial Cells, Nanomedicine, and Biotechnology* **44** 410–22
[13] Parveen S, Misra R and Sahoo S K 2012 Nanoparticles: a boon to drug delivery, therapeutics, diagnostics and imaging *Nanomed. Nanotechnol. Biol. Med.* **8** 147–66
[14] Patra S, Mukherjee S, Barui A K, Ganguly A, Sreedhar B and Patra C R 2015 Green synthesis, characterization of gold and silver nanoparticles and their potential application for cancer therapeutics *Mater. Sci. Eng. C* **53** 298–309
[15] Shilo M, Sharon A, Baranes K, Motiei M, Lellouche J-P M and Popovtzer R 2015 The effect of nanoparticle size on the probability to cross the blood-brain barrier: an *in-vitro* endothelial cell model *Journal of Nanobiotechnology* **13** 19
[16] Li J, Li J E J, Zhang J, Wang X, Kawazoe N and Chen G 2016 Gold nanoparticle size and shape influence on osteogenesis of mesenchymal stem cells *Nanoscale* **8** 7992–8007
[17] Corzo Lucioni A 2012 Síntesis de nanopartículas de oro obtenidas por reducción de H[$AuCl_4$] *Revista de la Sociedad Química del Perú* **78** 79–90
[18] Tseng K-H, Hsieh C-L, Huang J-C and Tien D-C 2015 The effect of NaCl/pH on colloidal nanogold produced by pulsed spark discharge *J. Nanomater.* **2015** 612324
[19] Cornejo-Monroy D, Sánchez-Santamaria B, Martínez-Gómez E A, Olivas-Armendáriz I, Villanueva-Montellano A, Arias-Cerón J S and Castaño V M 2019 Facile synthesis of ultrasmall, highly stable, and biocompatible gold nanoparticles stabilized with lipoic acid: cytotoxicity and structural characterization *Nanotechnol Russia* **14** 607–12

[20] Mondragón R, Juliá J E, Barba A and Jarque J C 2014 Preparación y caracterización de nanofluidos: influencia de variables sobre su estabilidad, estado de aglomeración y propiedades físicas *Bol. Soc. Esp. Ceram. Vidr.* **53** 101–10
[21] Ramdayal and Balasubramanian K 2014 Antibacterial application of polyvinylalcohol-nanogold composite membranes *Colloids Surf., A* **455** 174–8
[22] Yang Y, Matsubara S, Nogami M and Shi J 2007 Controlling the aggregation behavior of gold nanoparticles *Materials Science and Engineering: B* **140** 172–6
[23] Haiss W, Thanh N T K, Aveyard J and Fernig D G 2007 Determination of size and concentration of gold nanoparticles from UV–vis spectra *Anal. Chem.* **79** 4215–21
[24] Martínez J C, Chequer N A, González J L and Cordova T 2012 Alternative metodology for gold nanoparticles diameter characterization using PCA technique and UV–vis spectrophotometry *Nanoscience and Nanotechnology* **2** 184–9
[25] Hermanson G T 2013 *Bioconjugate Techniques* 3rd ed. (Rockford: Academic) 1200
[26] Meeker W Q and Escobar L A 1998 *Statistical Methods for Reliability Data* 1st ed. (New York, NY: Wiley) 712
[27] Liao H and Elsayed E A 2006 Reliability inference for field conditions from accelerated degradation testing *Naval Research Logistics (NRL)* **53** 576–87
[28] Wang X 2010 Wiener processes with random effects for degradation data *J. Multivariate Anal.* **101** 340–51
[29] Whitmore G A, Crowder M J and Lawless J F 1998 Failure inference from a marker process based on a bivariate Wiener model *Lifetime Data Anal.* **4** 229–51
[30] Ye Z-S, Shen Y and Xie M 2012 Degradation-based burn-in with preventive maintenance *Eur. J. Oper. Res.* **221** 360–7
[31] Li J, Wang Z, Zhang Y, Fu H, Liu C and Krishnaswamy S 2017 Degradation data analysis based on a generalized Wiener process subject to measurement error *Mech. Syst. Sig. Process.* **94** 57–72
[32] Peng C-Y and Tseng S-T 2009 Mis-specification analysis of linear degradation models *IEEE Trans. Reliab.* **58** 444–55
[33] Si X-S, Wang W, Hu C-H, Chen M-Y and Zhou D-H 2013 A Wiener-process-based degradation model with a recursive filter algorithm for remaining useful life estimation *Mech. Syst. Sig. Process.* **35** 219–37
[34] Si X-S, Wang W, Hu C-H, Zhou D-H and Pecht M G 2012 Remaining useful life estimation based on a nonlinear diffusion degradation process *IEEE Trans. Reliab.* **61** 50–67
[35] Tsai C-C, Tseng S-T and Balakrishnan N 2011 Mis-specification analyses of gamma and Wiener degradation processes *J. Stat. Plan. Inference* **141** 3725–35
[36] Sun L, Gu X and Song P 2016 Accelerated degradation process analysis based on the nonlinear Wiener process with covariates and random effects *Mathematical Problems in Engineering* **2016** 5246108
[37] Nocedal J 1980 Updating quasi-Newton matrices with limited storage *Math. Comput.* **35** 773–82
[38] Nguyen K T P, Fouladirad M and Grall A 2018 Model selection for degradation modeling and prognosis with health monitoring data *Reliab. Eng. Syst. Saf.* **169** 105–16
[39] Hesterberg T C 1999 *Bootstrap tilting confidence intervals* 84 Research Department, MathSoft, Inc., 1700 Westlake Ave. N., Suite 500, Seattle, WA 98109
[40] Cavanaugh J E and Neath A A 2019 The Akaike information criterion: background, derivation, properties, application, interpretation, and refinements *WIREs Computational Statistics* **11** e1460
[41] Wang Z, Li J, Ma X, Zhang Y, Fu H and Krishnaswamy S 2017 A generalized Wiener process degradation model with two transformed time scales *Qual. Reliab. Eng. Int.* **33** 693–708
[42] Li J, Wang Z, Liu X, Zhang Y, Fu H and Liu C 2016 A Wiener process model for accelerated degradation analysis considering measurement errors *Microelectron. Reliab.* **65** 8–15
[43] Jain A K, Dubes R C and Chen C-C 1987 Bootstrap techniques for error estimation *IEEE Trans. Pattern Anal. Mach. Intell.* **PAMI-9** 628–33